

# Pristimerin Inhibits MMP-9 Expression and Cell Migration Through Attenuating NOX/ROS-Dependent NF- $\kappa$ B Activation in Rat Brain Astrocytes Challenged with LPS

This article was published in the following Dove Press journal:  
*Journal of Inflammation Research*

Chien-Chung Yang<sup>1,2</sup>  
Li-Der Hsiao<sup>3</sup>  
Hui-Ching Tseng<sup>3</sup>  
Ching-Ming Kuo<sup>3</sup>  
Chuen-Mao Yang<sup>3,4</sup>

<sup>1</sup>Department of Traditional Chinese Medicine, Chang Gung Memorial Hospital at Tao-Yuan, Tao-Yuan 33302, Taiwan;

<sup>2</sup>School of Traditional Chinese Medicine, College of Medicine, Chang Gung University, Tao-Yuan 33302, Taiwan;

<sup>3</sup>Department of Pharmacology, College of Medicine, China Medical University, Taichung 40402, Taiwan; <sup>4</sup>Department of Post-Baccalaureate Veterinary Medicine, College of Medical and Health Science, Asia University, Taichung 41354, Taiwan

**Purpose:** Neuroinflammation plays a crucial role in neurodegenerative diseases. Matrix metalloproteinases (MMPs) are a landmark of neuroinflammation. Lipopolysaccharide (LPS) has been demonstrated to induce MMP-9 expression. The mechanisms underlying LPS-induced MMP-9 expression have not been completely elucidated in astrocytes. Nuclear factor-kappaB (NF- $\kappa$ B) is well known as one of the crucial transcription factors in MMP-9 induction. Moreover, reactive oxygen species (ROS) could be an important mediator of neuroinflammation. Here, we differentiated whether ROS and NF- $\kappa$ B contributed to LPS-mediated MMP-9 expression in rat brain astrocytes (RBA-1). Besides, pristimerin has been revealed to possess antioxidant and anti-inflammatory effects. We also evaluated the effects of pristimerin on LPS-induced inflammatory responses.

**Methods:** RBA-1 cells were used for analyses. Pharmacological inhibitors and siRNAs were used to evaluate the signaling pathway. Western blotting and gelatin zymography were conducted to evaluate protein and MMP-9 expression, respectively. Real-time PCR was for mRNA expression. Wound healing assay was for cell migration. 2',7'-dichlorodihydrofluorescein diacetate (H<sub>2</sub>DCF-DA) and dihydroethidium (DHE) staining were for ROS generation. Immunofluorescence staining was conducted to assess NF- $\kappa$ B p65. Promoter-reporter gene assay and chromatin immunoprecipitation (ChIP) assay were used to detect promoter activity and the association of nuclear proteins with the promoter.

**Results:** Our results showed that the increased level of ROS generation was attenuated by edaravone (a ROS scavenger), apocynin (APO; an inhibitor of p47<sup>Phox</sup>), diphenyleneiodonium (DPI; an inhibitor of NOX), and pristimerin in RBA-1 cells exposed to LPS. Besides, pretreatment with APO, DPI, edaravone, Bay11-7082, and pristimerin also inhibited the phosphorylation, nuclear translocation, promoter binding activity of NF- $\kappa$ B p65 as well as upregulation of MMP-9 expression-mediated cell migration in RBA-1 cells challenged with LPS.

**Conclusion:** These results suggested that LPS enhances the upregulation of MMP-9 through nicotinamide adenine dinucleotide phosphate (NADPH) oxidase (NOX)/ROS-dependent NF- $\kappa$ B activity. These results also provide new insights into the mechanisms by which pristimerin attenuates LPS-mediated MMP-9 expression and neuroinflammatory responses.

**Keywords:** neuroinflammation, NOX, ROS, LPS, MMP-9, pristimerin, astrocytes

## Introduction

Astrocytes are considered as a group of neural cells of ectodermal and neuroepithelial origin, which maintain homeostasis and provide for the defense of the central

Correspondence: Chuen-Mao Yang  
Tel +886 4-22053366 (Ext. 2229)  
Email chuenmao@mail.cmu.edu.tw

nervous system (CNS). When oxidative stress elicited by inflammatory reactions in the CNS, astroglia were suffered from a variety of harmful effects caused by the elevated levels of reactive oxygen species (ROS).<sup>1</sup> In CNS, the nicotinamide adenine dinucleotide phosphate (NADPH) oxidase (NOX) is recognized as an enzymatic origin of ROS synthesis contributing to detrimental effects under various physio-pathological conditions.

Lipopolysaccharide (LPS), known as the main part of the outer membrane of Gram-negative bacteria, is the negatively charged glycolipid which provides the structural integrity and stabilization of the bacteria. LPS binds with the cluster of differentiation (CD)14/Toll-like receptor (TLR)4/lymphocyte antigen 96 (MD2) receptor complex to activate a series of signaling pathways in many types of cells, which in turn promotes the expression of inflammatory mediators. Recently, some reports have indicated that LPS participates in the pathogenesis of neurodegeneration.<sup>2</sup> Several animal models of neurodegenerative disorders have shown that pure inflammation by LPS administration can induce nigrostriatal dopaminergic neurodegeneration<sup>3</sup> or memory impairment for Alzheimer's disease (AD).<sup>4,5</sup> The mechanisms underlying LPS-triggered neuronal death are mediated through TLR4 activating microglia and astrocytes, which induce the release of proinflammatory cytokines, chemokines, and complement system proteins. In turn, these proinflammatory mediators enhance ROS generation causing neuronal damage. Another study also proposed that LPS could be a risk factor of sporadic AD because Gram-negative *Escherichia coli* (*E. coli*) bacteria can form extracellular amyloid; blood levels of LPS are 3-fold in AD patients compared with control; microbes have been demonstrated in erythrocytes of AD patients; and LPS produces amyloid-like plaques in adult rat cortex.<sup>6</sup> Growing evidence indicates that endotoxin stimulates tau and amyloid  $\beta$  (A $\beta$ ) aggregation, and colocalizes with A $\beta$ 1-40/42 in amyloid plaques and around vessels in AD brain,<sup>7</sup> indicating that endotoxin synergies with various aggregable proteins to contribute to unique neurodegenerative diseases.<sup>8,10</sup> On the other hand, several reports have revealed that LPS can trigger matrix metalloproteinase (MMP)-9 expression in numerous types of cells.<sup>11,12</sup> Upregulation of MMP-9 can cause blood-brain barrier (BBB) damage leading to hemorrhagic transformation, neuronal damage, excitotoxicity, apoptosis as well as cerebral edema. Therefore, MMP-9 is well known as an important inflammatory factor involved in numerous neurodegenerative diseases such

as AD, stroke, and multiple sclerosis.<sup>13,15</sup> Although we have demonstrated that in RBA-1 cells, the TLR4/c-Src/Pyk2/PDGFR/PI3K/Akt/p38 MAPK and JNK1/2-dependent activation of AP-1 can mediate LPS-induced MMP-9 expression,<sup>11</sup> whether alternative pathways such as NOX/ROS-dependent nuclear factor kappaB (NF- $\kappa$ B) were involved in LPS-induced responses were still unknown.

Pristimerin is one of the triterpenoids, which exhibits many pharmacological effects, such as anti-microbe, anti-peroxidation, anti-inflammation, and inhibiting tumor angiogenesis.<sup>16,18</sup> Pristimerin can inhibit LPS-triggered neurotoxicity through attenuating interleukin-1 receptor-associated kinase (IRAK1)/TNF receptor-associated factor 6 (TRAF6)/TGF- $\beta$  activating kinase 1 (TAK1)-mediated activator protein-1 (AP-1) and NF- $\kappa$ B signaling pathways in BV-2 microglial cells.<sup>17</sup> Deng et al. also demonstrated that pristimerin significantly reduces the expression of pro-angiogenic factors in sera, including tumor necrosis factor (TNF)- $\alpha$ , angiopoietin-1 (Ang-1), and MMP-9 and angiogenesis in synovial membrane tissues of inflamed joints.<sup>16</sup> Another study also showed that the administration of pristimerin significantly reduces the formation of MMP-9 and oxidative stress induced by doxorubicin through the inhibition of NF- $\kappa$ B signaling in cardiotoxicity model of rat.<sup>19</sup> However, the mechanisms underlying the anti-inflammatory effects of pristimerin on MMP-9 expression remain unknown in RAB-1 cells.

In this study, we dissected the signaling components linking NF- $\kappa$ B activation induced by LPS to MMP-9 expression and the effects of pristimerin on LPS-mediated responses in RBA-1 cells. Our results demonstrated that NOXs/ROS generation-dependent activation of NF- $\kappa$ B mediates LPS-induced MMP-9 expression, leading to RBA-1 cell migration. Moreover, pristimerin inhibited MMP-9 expression associated with cell migration through attenuating NOXs/ROS-dependent NF- $\kappa$ B activation in RBA-1 cells challenged with LPS.

## Materials and Methods

### Antibodies and Inhibitors

Dulbecco's modified Eagle's medium (DMEM)/Ham's nutrient mixture F-12 (F-12), fetal bovine serum (FBS), and siRNAs for NF- $\kappa$ B p65 (RSS317830), NOX1 (RSS300165), NOX2 (RSS330363), and p47<sup>phox</sup> (RSS300253) were purchased from Invitrogen (Carlsbad, CA, USA). Hybond C membrane and enhanced

chemiluminescence (ECL) detection system were purchased from GE Healthcare Biosciences (Buckinghamshire, UK). Anti-phospho NF- $\kappa$ B p65 (Ser536, #3033) and anti-NF- $\kappa$ B p65 (#8242) antibodies were purchased from Cell Signaling (Danvers, MA, USA). Anti-glyceraldehyde-3-phosphate dehydrogenase (GAPDH) (#MCA-ID4) was purchased from EnCor (Gainesville, FL). All primary antibodies were diluted at 1:1000 in phosphate-buffered saline (PBS) with 1% bovine serum albumin (BSA). H<sub>2</sub>DCFDA and dihydroethidium (DHE) were purchased from Thermo Fisher Scientific (Waltham, Massachusetts, USA). Apocynin (APO), diphenyleioidonium (DPI), and Bay11-7082 were purchased from Biomol (Plymouth Meeting, PA, USA). Edaravone was purchased from Tocris Bioscience (Bristol, UK). Bicinchoninic acid (BCA) protein assay reagent was purchased from Pierce (Rockford, IL, USA). Sodium dodecyl sulfate-polyacrylamide gel electrophoresis (SDS-PAGE) reagents were purchased from MDBio Inc (Taipei, Taiwan). Dimethyl sulfoxide (DMSO), enzymes, TRIzol, [2,3-bis-(2-methoxy-4-nitro-5-sulfophenyl)-2H-tetrazolium-5-carboxanilide] (XTT) assay kit, and other chemicals were purchased from Sigma (St. Louis, MO, USA). Pristimerin was purchased from Cayman Chemicals (Ann Arbor, MI, USA).

## Cell Culture and Treatment

In this study, RBA-1 cells were originated from primary cultured astrocytes of neonatal rat cerebrum and naturally developed through successive cell passages.<sup>11,20</sup> The use of the cell lines had been approved by Chang Gung University Institutional Animal Care and Use Committee (IACUC Approval No.: CGU16-081). The anti-gial fibrillary acidic protein (GFAP) antibody, an astrocyte-specific marker, was used to assess the purity of cultured astrocytes. GFAP-positive astrocytes were shown over 95%. Cells from passages 4 to 35 were used throughout these experiments. An XTT assay was used to assay the cytotoxicity of LPS and pharmacological inhibitors at the incubation time, showing no significant effect on cell viability. The cells were plated on 6-well (2 mL/well) or 12-well (1 mL/well) culture plates. The cells were starved by incubation in serum-free DMEM/F-12 for 24 h, and then incubated with LPS at 37 °C for the indicated time intervals. Upon the inhibitors used, they were added 1 h prior to the exposure to LPS.

## Protein Preparation and Western Blotting

The cells were washed with ice-cold PBS and added with SDS-loading buffer (0.1 M Tris-HCl of pH 6.8, 1% SDS,

5% glycerol, 2.5%  $\beta$ -mercaptoethanol, and 0.02% bromophenol blue). Proteins were separated by SDS-PAGE and transferred onto Hybond-C membranes. Protein level was detected by primary antibodies diluted at 1:1000 in Tween-Tris-buffered saline (TTBS)<sup>11,21</sup> and a secondary horseradish peroxidase-conjugated antibody diluted at 1:1500. An anti-GAPDH antibody was used as an internal control. The membranes were incubated with a secondary antibody for 1 h after washed with TTBS four times for 30 min each. Following incubation, the membranes were extensively washed with TTBS. The immunoreactive bands were detected by enhanced chemiluminescence (ECL) reagents and captured by a UVP BioSpectrum 500 Imaging System (Upland, CA, USA). The image densitometry analysis was conducted using UN-SCAN-IT gel software (Orem, UT, USA).

## MMP Gelatin Zymography

Growth-arrested cells were challenged by LPS for the indicated time intervals. The culture media were collected and centrifuged at 1000 $\times$  g for 10 min at 4 °C to remove the cells and debris. Following centrifuging, the samples under non-reducing conditions were electrophoretically separated on 10% SDS-PAGE copolymerized with 1 mg/mL gelatin (Sigma-Aldrich, St. Louis, MS, USA), as described previously.<sup>11,21</sup> To remove SDS, 2.5% Triton X-100 washed the gels twice; then the gels were incubated for 72 h with a developing buffer containing 50 mM Tris, 40 mM HCl, 200 mM NaCl, 5 mM CaCl<sub>2</sub>, and 0.02% Brij-35 at 37 °C. The gels were stained in 30% methanol, 10% acetic acid, and 0.5% w/v Coomassie Blue R-250 for 1 h, and followed by being de-stained to visualize the gelatinolytic bands (MMP-9) on a dark blue background. A mixed human MMP-2 and MMP-9 (Chemicon, Temecula CA, USA) was used for gelatinase standards. Because cleaved MMPs are not reliably detectable, only pro-form zymogens were quantified in this study.

## Transient Transfection with siRNA

As previously described,<sup>11</sup> 2  $\times$  10<sup>5</sup> RBA-1 cells/mL were plated onto 6-well plates. While cells were reaching about 70% confluence, cells were washed once with PBS and incubated with 1 mL/well of DMEM/F-12 with 5% FBS before transfection. Genmute transfection reagent (SignaGen Laboratories, Rockville, MD, USA) was used to carry out the transient transfection of siRNA. The transfection reagent complexes contained siRNA with a final concentration of 50 nM were added to each well and then incubated at 37 °C

for 5 h. The cells were incubated with fresh DMEM/F-12 with 5% FBS for an additional 8 h. The cells were washed twice with PBS and then maintained in serum-free DMEM/F-12 for 16 h, and then challenged with LPS.

## Total RNA Extraction and Real-Time PCR Analysis

Total RNA was extracted from RBA-1 cells, as previously described.<sup>11,21</sup> mRNA was reverse-transcribed into cDNA and analyzed by real-time quantitative PCR (RT-qPCR). Based on Genbank entries for rat MMP-9 and GAPDH, the oligonucleotide primers were designed. The following primers were used for amplification reaction:

MMP-9:

5'-AGTTTGGTGTGCGGAGCAC-3' (sense);

5'-TACATGAGCGCTCCGGCAC-3' (antisense);

5'-CGCTCTGCATTTCTTCAAGGACGGT-3'-tetra-

methylrhodamine (TAMRA, Probe)

GAPDH:

5'-(AAGTTTGGCATCGTGGAAGG)-3' (sense);

5'-(GTGGATGCAGGGATGATGTTT)-3' (antisense);

5'-TGACCACAGTCCATGCCATCACTGC-3'-TAMRA

(Probe).

RT-qPCR was performed with a StepOnePlus™ Real-Time PCR System (ThermoScientific-Applied Biosystems, San Mateo, CA, USA) and Kapa Probe Fast qPCR Kit Master Mix Universal (KK4705; KAPA Biosystems, Wilmington, MA, USA). The levels of MMP-9 expression were quantified by normalization to the GAPDH expression. Relative gene expression was determined by using the  $\Delta\Delta C_t$  method, where  $C_t$  = threshold cycle. All experiments were performed in triplicate.

## Rat MMP-9 Promoter Reporter Gene Assay

The upstream region (-1280 to +108) of the rat MMP-9 promoter was cloned into pGL3-basic vector containing the luciferase reporter system.<sup>11,22</sup> The constructs of MMP-9-luciferase and  $\kappa B$ -luciferase (Clontech) were produced by QIAGEN plasmid DNA preparation kits. The construct was transfected into RBA-1 cells using a Lipofectamine reagent. For the control of transfection efficiencies, a pGal (a plasmid) encoding for  $\beta$ -galactosidase was used to transfect. The cells were incubated with LPS, collected, and disrupted by sonication in a lysis buffer (25 mM Tris-phosphate, pH 7.8, 2 mM EDTA, 1% Triton X-100, and

10% glycerol) to determine the promoter activity using a luciferase assay system (Abcam, Cambridge, United Kingdom). Finally, luciferase activities were standardized to  $\beta$ -gal activity.

## Cell Migration Assay

RBA-1 cells were plated onto 6-well culture plates to grow confluence and starved with serum-free DMEM/F-12 medium for 24 h. The cells were manually scratched a bright and clear field (about 2 mm) in the center of the monolayer cells each well, as previously described.<sup>11</sup> The cells were washed once with PBS to remove the detached cells. Serum-free DMEM/F-12 medium with or without LPS (2  $\mu$ g/mL) and the DNA synthesis inhibitor hydroxyurea (10  $\mu$ M) was added to each dish during the period of observation as indicated after pretreatment with or without each inhibitor for 1 h. Migrating cells from the scratch boundary were observed under a light microscope and imaged with a digital camera (Olympus, Japan). The data demonstrated were summarized from three individual experiments.

## Chromatin Immunoprecipitation (ChIP) Assay

Chromatin immunoprecipitation analysis was conducted to detect the association of nuclear proteins with rat MMP-9 promoter as previously described.<sup>11</sup> Briefly, RBA-1 cells were cross-linked with 1% formaldehyde for 10 min at 37°C and then washed thrice with ice-cold PBS containing 1 mM phenylmethylsulfonyl fluoride (PMSF) and 1% aprotinin. The cell lysates were collected in a SDS-lysis buffer (1% SDS, 5mM EDTA, 1 mM PMSF, 50 mM Tris-HCl) and then sonicated at 4°C until the DNA size became 200–300 base pairs. The soluble chromatin was incubated with sheared salmon sperm DNA-protein agarose A to the preclear. One portion of the supernatant was used as a DNA input control, and the other was immunoprecipitated with an anti-p65 antibody and protein A beads. Following washing and elution, precipitates were heated at 65°C overnight to reverse the cross-linking of DNA and protein. DNA fragments were purified by phenol-chloroform extraction and ethanol precipitation. The purified DNA was subjected to PCR amplification using the primers specific for the region (-606 to -327, accession no. AF148065) containing the NF- $\kappa B$  binding elements located in the MMP-9 promoter region. The primers included a sense primer: 5'-AGAGCCTGCTCCCAGAGGGC-3' and an anti-sense primer: 5'-GCCAAGTCAGGCA GGACCCC-3'. PCR

fragments were analyzed by 3% agarose in  $1\times$  TAE gel containing ethidium bromide. The size (280 bp) of PCR products was ensured by comparing it with a molecular weight marker.

## Immunofluorescence Staining

Growth-arrested cells were treated with LPS (2  $\mu\text{g}/\text{mL}$ ) for the indicated time intervals. After washing twice with ice-cold PBS, cells were fixed, permeabilized, stained using anti-p65 antibodies (1:200 dilutions) and 4',6-diamidino-2-phenylindole (DAPI), and finally mounted as previously described.<sup>23</sup> The images were observed with a fluorescence microscope (Zeiss, Axiovert 200 M).

## Measurement of Intracellular ROS Accumulation

The fluorescence of  $\text{H}_2\text{DCF-DA}$  and DHE was used to determine the levels of intracellular  $\text{H}_2\text{O}_2$  and  $\text{O}_2^-$ . Six-well culture plates with coverslips were used in these experiments. The growth-arrested cells were challenged with LPS with/without pretreatment with inhibitors or pristinerin for the indicated time intervals (5, 10, and 30 min). For  $\text{H}_2\text{DCF-DA}$  staining, the cells were incubated in PBS containing 10  $\mu\text{M}$   $\text{H}_2\text{DCF-DA}$  at  $37^\circ\text{C}$  for 30 min, washed twice with warm PBS, incubated in fresh medium, and then observed using a fluorescence microscope (Zeiss, Axiovert 200M). In addition, the cells were incubated with DHE at a final concentration of 5  $\mu\text{M}$  for 30 min at  $37^\circ\text{C}$ . Subsequently, the cells were washed out three times with PBS to remove DHE and replaced with the fresh medium. Following cells washed, a fluorescence microscope was used to observe the resulting fluorescence.

## Statistical Analysis of Data

A GraphPad Prism Program (GraphPad, San Diego, CA, USA) was used to estimate all the data. Data were expressed as the mean  $\pm$  SEM and analyzed by one-way analysis of variance (ANOVA) followed by Tukey's post hoc test.  $p < 0.01$  was considered significant.

## Results

### LPS-Induced MMP-9 Expression and Cell Migration Are Mediated Through ROS Generation

ROS are recognized as important signaling components in the regulation of inflammatory responses.<sup>1</sup> Several pieces of research have demonstrated that ROS have pivotal roles in neuroinflammation including LPS-triggered responses.<sup>24,26</sup>

First, we explored the function of ROS in LPS-induced MMP-9 expression. Edaravone, known to be an antioxidant, was used for this purpose. We found that pretreatment with edaravone (1, 10, and 30  $\mu\text{M}$ ) dose-dependently inhibited LPS-induced MMP-9 expression in RBA-1 cells (Figure 1A). The levels of promoter activity and MMP-9 mRNA induced by LPS were also attenuated by pretreatment with edaravone (30  $\mu\text{M}$ ) (Figure 1B). To determine whether ROS generation was required for the LPS-induced MMP-9 expression, we observed that LPS stimulated ROS generation in a time-dependent manner (Figure 1C), which was attenuated by pretreatment of RBA-1 cells with edaravone (Figure 1D), revealed by DCFH-DA or dihydroethidium (DHE) staining. Finally, pretreatment with 30  $\mu\text{M}$  edaravone blocked the upregulation of MMP-9-mediated cell migration in RBA-1 cells triggered by LPS (Figure 1E). These results indicated that ROS participates in LPS-mediated MMP-9 expression and cell migration in RBA-1 cells.

### NADPH Oxidase Is Involved in MMP-9 Expression and Cell Migration Induced by LPS

Several studies have demonstrated that LPS-mediated MMP-9 expression is mediated through NOX1 and NOX2 activity.<sup>24,27,28</sup> NOX is the major source for ROS generation which acts as second messengers to stimulate the expression of inflammatory proteins.  $\text{p47}^{\text{Phox}}$  has been shown to be a key player for the NOX activation and ROS generation. To investigate the role of  $\text{p47}^{\text{Phox}}$  in the LPS-mediated responses, an inhibitor of  $\text{p47}^{\text{Phox}}$  apocynin (APO) was used in these experiments. We found that pretreatment with APO attenuated the LPS-induced MMP-9 protein in a concentration-dependent manner in RBA-1 cells (Figure 2A). The levels of LPS-induced MMP-9 mRNA and promoter activity were also inhibited by pretreatment with APO (Figure 2B). To determine whether  $\text{p47}^{\text{Phox}}$  was directly involved in ROS generation, we observed that the LPS-stimulated ROS generation was inhibited by pretreatment with APO, as shown in staining with either  $\text{H}_2\text{DCF-DA}$  or DHE (Figure 2C). To verify the role of  $\text{p47}^{\text{Phox}}$  in LPS-induced responses, transfection of RBA-1 cells with  $\text{p47}^{\text{Phox}}$  siRNA knocked down the level of  $\text{p47}^{\text{Phox}}$  protein which caused the LPS-induced MMP-9 expression attenuated (Figure 2D). Moreover, pretreatment with APO or transfection with  $\text{p47}^{\text{Phox}}$  siRNA attenuated LPS-mediated cell migration (Figure 2E). These results

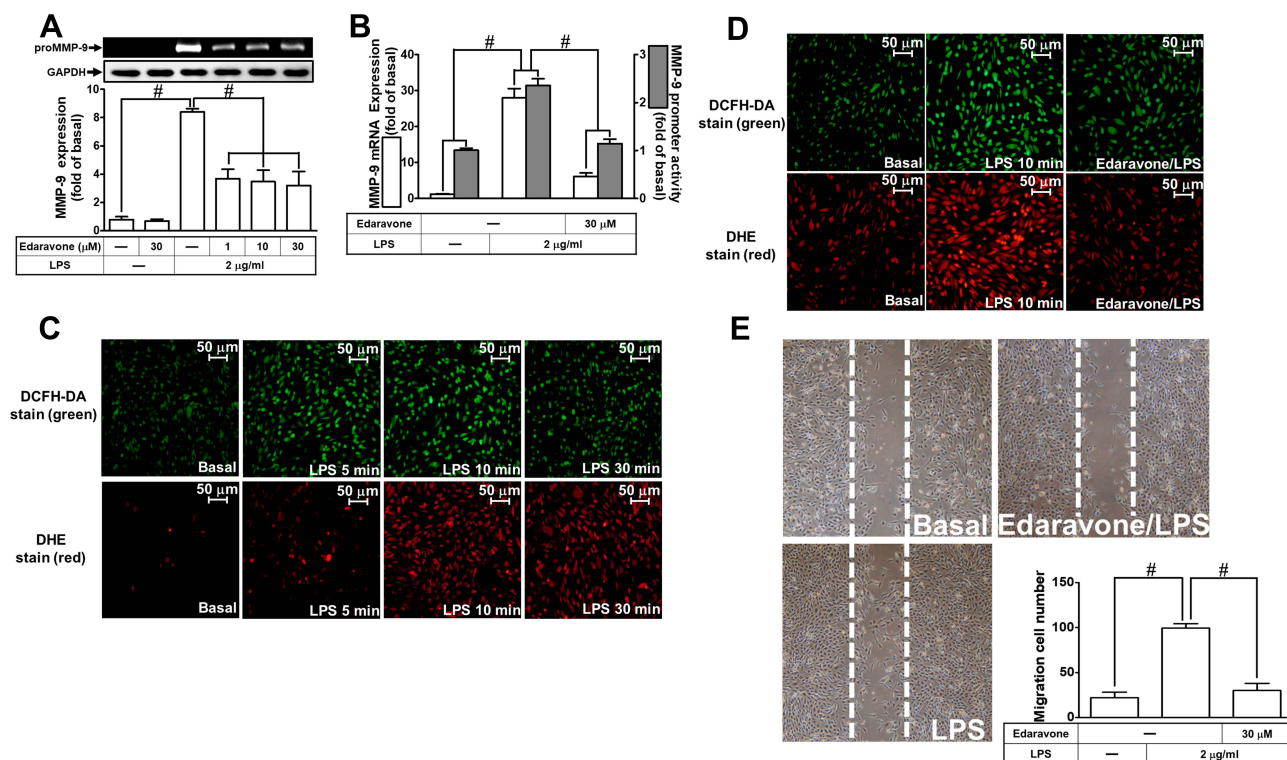


**Figure 1** Reactive oxygen species (ROS) are involved in lipopolysaccharide (LPS)-induced MMP-9 expression and cell migration in RBA-1 cells. **(A)** Cells were pretreated with edaravone (1, 10, and 30 μM) for 1 h and then stimulated with LPS (2 μg/mL) for 24 h. The levels of MMP-9 were examined by gelatin zymography. The GAPDH level of cell lysates was assayed by Western blot. **(B)** Cells were pretreated with edaravone (30 μM) for 1 h and then incubated with LPS (2 μg/mL) of 4 h for mRNA expression or 6 h for promoter activity. The mRNA expression and promoter activity of MMP-9 were determined by real-time PCR and promoter assay, respectively. **(C)** Cells were incubated with LPS (2 μg/mL) for the indicated time intervals (5, 10, and 30 min). Then, the fluorescence intensity of DCFH-DA or DHE staining was detected by a fluorescence microscope. The figure represents one of three individual experiments. Scale bar = 50 μm. **(D)** Cells were pretreated with or without edaravone (30 μM) for 1 h and then incubated with LPS (2 μg/mL) for 10 min. The fluorescence intensity of DCFH-DA or DHE staining was detected by a fluorescence microscope. The figure represents one of three individual experiments. Scale bar = 50 μm. **(E)** Cells were pretreated with or without edaravone (30 μM) for 1 h and then incubated with LPS (2 μg/mL) for 48 h. The number of cell migration was determined (magnification = 40×). Data are expressed as mean ± SEM of three independent experiments. #  $p < 0.01$  as compared with the cells exposed to vehicle or LPS, as indicated.

**Abbreviation:** GAPDH, glyceraldehyde 3-phosphate dehydrogenase.

suggested that p47<sup>Phox</sup>-dependent ROS generation mediates LPS-induced MMP-9 expression and cell migration in RBA-1 cells.

Further, we explored the role of NOX in LPS-induced ROS generation and MMP-9 expression. We found that pretreatment of RBA-1 cells with an inhibitor of NOX, diphenyleneiodonium (DPI), attenuated the LPS-induced MMP-9 protein (Figure 3A), mRNA, and promoter activity (Figure 3B). Moreover, it is well known that NOX plays a pivotally enzymatic resource of ROS generation. To investigate whether LPS-induced ROS generation was directly mediated through activated NOX, we observed that pretreatment with DPI attenuated LPS-enhanced ROS generation, determined by staining with either DCFH-DA or DHE (Figure 3C). These results suggested that NOX-dependent ROS generation can mediate LPS-induced MMP-9 expression in RBA-1 cells. NOX1 and 2 have been shown to express on

RBA-1 cells.<sup>29</sup> Thus, we further ensured whether NOX1 and 2 participated in the LPS-induced MMP-9 expression. We observed that transfection with either NOX1 or NOX2 siRNA knocked down the level of NOX1 or NOX2 which caused the LPS-induced MMP-9 expression attenuated (Figure 3D). Further, pretreatment with DPI (Figure 3E, left) or transfection with either NOX1 or NOX2 siRNA (Figure 3E, right) attenuated the upregulation of MMP-9 and cell migration induced by LPS. These results suggested that either NOX1 or NOX2 is involved in the LPS-mediated MMP-9 expression and cell migration in RBA-1 cells.

## LPS-Induced MMP-9 Expression Is Mediated via NF-κB P65 Signaling

NF-κB plays a pivotal role in MMP-9 expression in various types of cells through interaction with the promoter

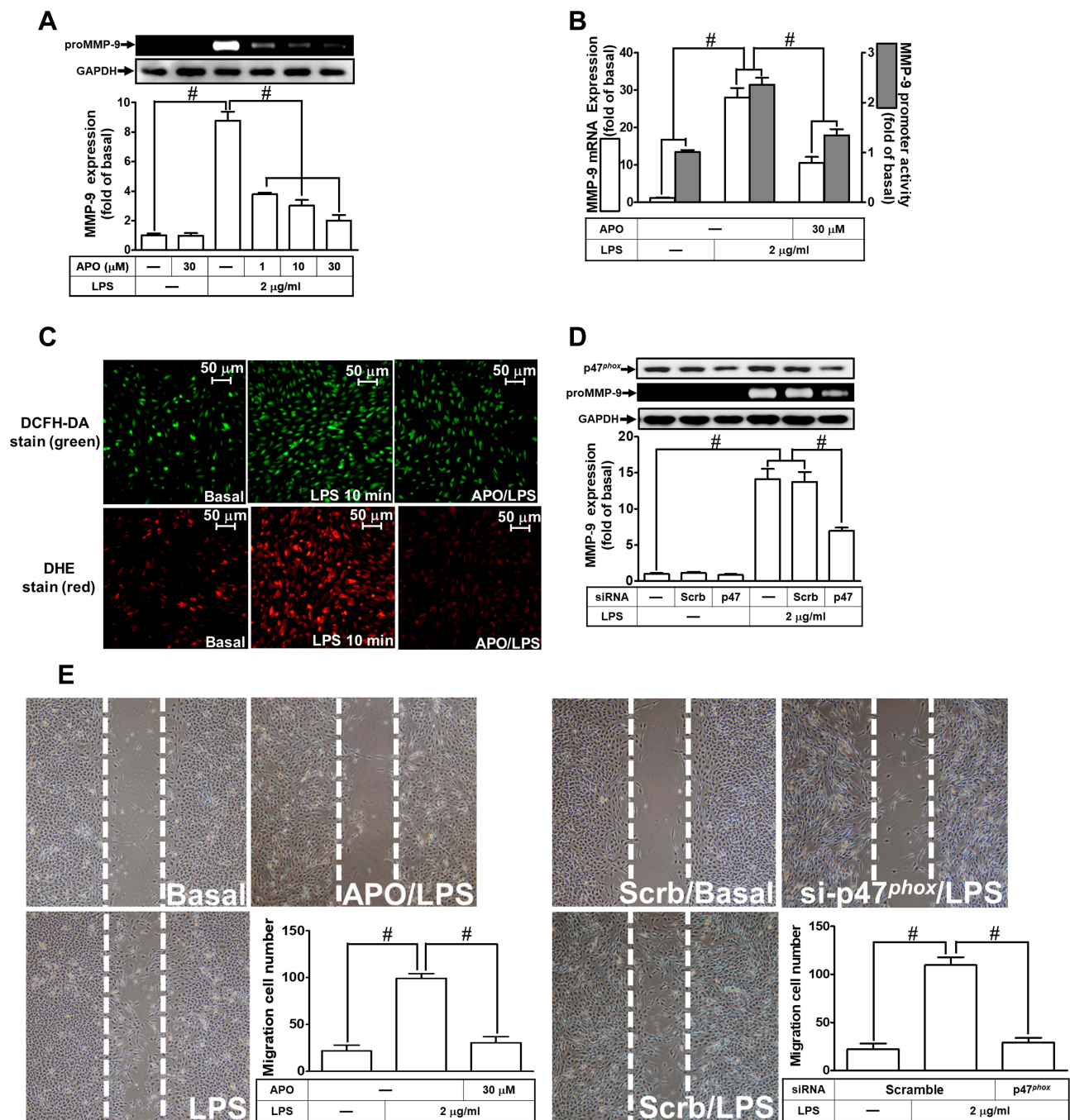


**Figure 2** P47<sup>phox</sup> is involved in lipopolysaccharide (LPS)-induced MMP-9 expression and cell migration in RBA-1 cells. **(A)** Cells were pretreated with apocynin (APO; 1, 10, and 30  $\mu\text{M}$ ) for 1 h and then incubated with LPS (2  $\mu\text{g/ml}$ ) for 24 h. The levels of MMP-9 were examined by gelatin zymography. The GAPDH level of cell lysates was assayed by Western blot. **(B)** Cells were pretreated with APO (30  $\mu\text{M}$ ) for 1 h and then incubated with LPS (2  $\mu\text{g/ml}$ ) of 4 h for mRNA expression or 6 h for promoter activity. The mRNA expression and promoter activity of MMP-9 were determined by real-time PCR and promoter assay, respectively. **(C)** Cells were pretreated with or without APO (30  $\mu\text{M}$ ) for 1 h and then incubated with LPS (2  $\mu\text{g/ml}$ ) for 10 min. The fluorescence intensity of DCFH-DA or DHE staining was detected by a fluorescence microscope. The figure represents one of three individual experiments. Scale bar = 50  $\mu\text{m}$ . **(D)** Cells were individually transfected with scrambled (Scrb) or p47<sup>phox</sup> siRNA and then incubated with LPS (2  $\mu\text{g/ml}$ ) for 24 h. The medium and cell lysates were collected to determine the levels of MMP-9 by gelatin zymography and the levels of GAPDH and p47<sup>phox</sup> by Western blot, respectively. **(E)** Cells were pretreated with or without APO (30  $\mu\text{M}$ ) for 1 h (left panel), and transfected with Scrb or p47<sup>phox</sup> siRNA (right panel) and then incubated with LPS (2  $\mu\text{g/ml}$ ) for 48 h. The number of cell migration was determined (magnification = 40 $\times$ ). Data are expressed as mean  $\pm$  SEM of three independent experiments. #  $p < 0.01$  as compared with the cells exposed to vehicle or LPS, as indicated.

region of MMP-9.<sup>30</sup> Thus, in RBA-1 cells, we evaluated the role of NF- $\kappa$ B in the LPS-mediated MMP-9 expression. First, we found that pretreatment of RBA-1 cells with

Bay11-7082 (0.01, 0.1, and 1  $\mu\text{M}$ ) inhibited the LPS-induced MMP-9 expression in a dose-dependent manner (Figure 4A). Pretreatment with Bay11-7082 (1  $\mu\text{M}$ ) also

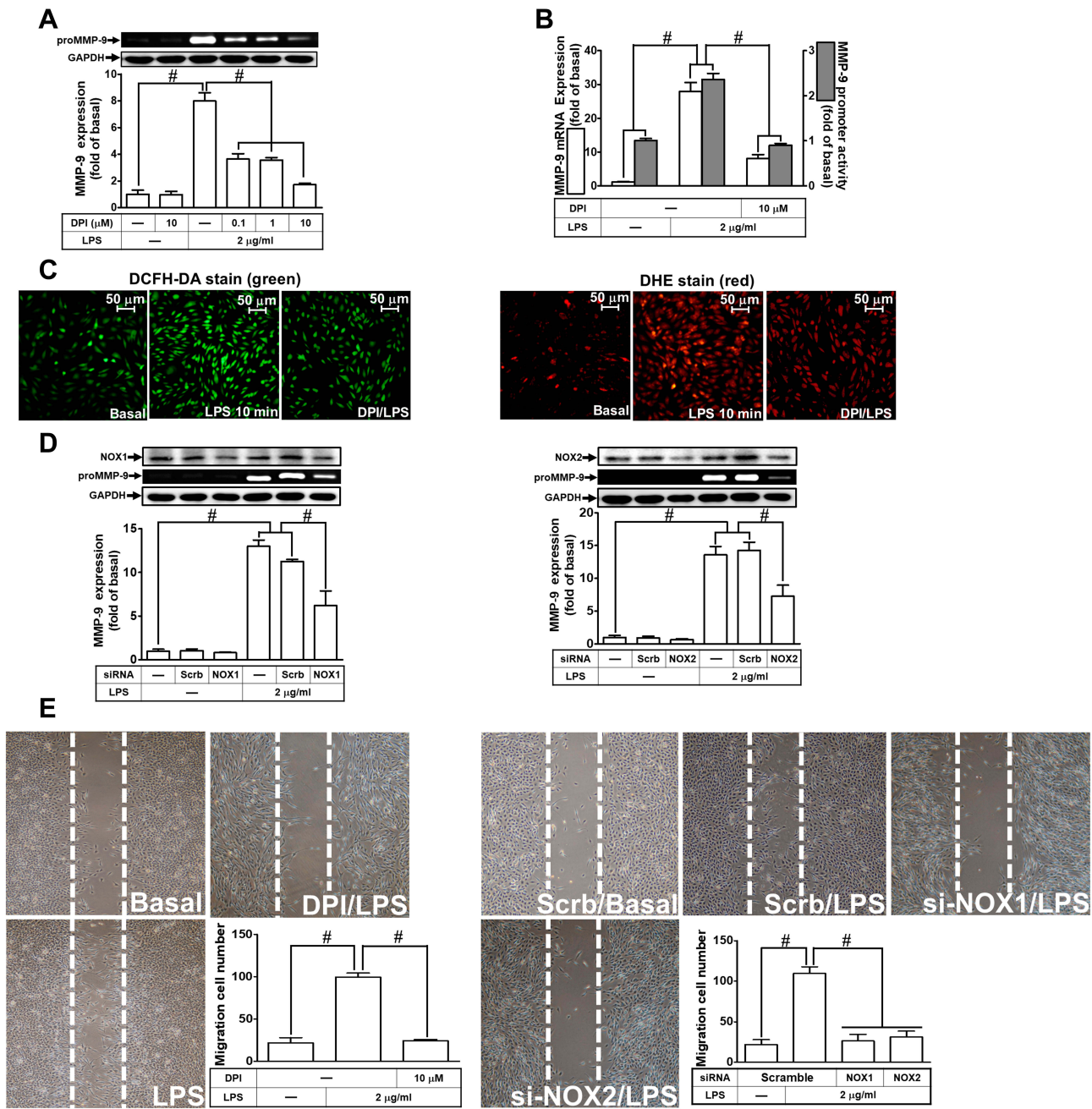


**Figure 3** Nicotinamide adenine dinucleotide phosphate (NADPH) oxidase (NOX) is involved in lipopolysaccharide (LPS)-induced MMP-9 expression and cell migration in RBA-1 cells. **(A)** Cells were pretreated with diphenyleioidonium (DPI: 0.1, 1, and 10  $\mu$ M) for 1 h and then stimulated with LPS (2  $\mu$ g/mL) for 24 h. The levels of MMP-9 were examined by gelatin zymography. The GAPDH level of cell lysates was assayed by Western blot. **(B)** Cells were pretreated with DPI (10  $\mu$ M) for 1 h and then incubated with LPS (2  $\mu$ g/mL) for 4 h for mRNA expression or 6 h for promoter activity. The mRNA expression and promoter activity of MMP-9 were determined by real-time PCR and promoter assay, respectively. **(C)** Cells were pretreated with or without DPI (10  $\mu$ M) for 1 h and then incubated with LPS (2  $\mu$ g/mL) for 10 min. The fluorescence intensity of DCFH-DA or DHE staining was detected by a fluorescence microscope. The figure represents one of three individual experiments. Scale bar = 50  $\mu$ m. **(D)** Cells were transfected with scrambled (Scrb), NOX1 or NOX2 siRNA and then incubated with LPS (2  $\mu$ g/mL) for 24 h. The medium and cell lysates were collected to determine the levels of MMP-9 by gelatin zymography and the levels of GAPDH, NOX1, and NOX2 by Western blot, respectively. **(E)** Cells were pretreated with or without DPI (10  $\mu$ M) for 1 h, or transfected with Scrb, NOX1 or NOX2 siRNA and then incubated with LPS (2  $\mu$ g/mL) for 48 h. The number of cell migration was determined (magnification = 40 $\times$ ). Data are expressed as mean  $\pm$  SEM of three independent experiments. #  $p < 0.01$  as compared with the cells exposed to vehicle or LPS, as indicated.

inhibited the levels of MMP-9 mRNA and promoter activity in these cells (Figure 4B). To verify the role of NF- $\kappa$ B in MMP-9 expression, as shown in Figure 4C, the LPS-induced MMP-9 expression was inhibited by transfection

with NF- $\kappa$ B p65 siRNA knocking down the level of NF- $\kappa$ B p65 protein in RBA-1 cells. Moreover, pretreatment with Bay11-7082 blocked cell migration of RBA-1 triggered by LPS (Figure 4D). These results suggested that



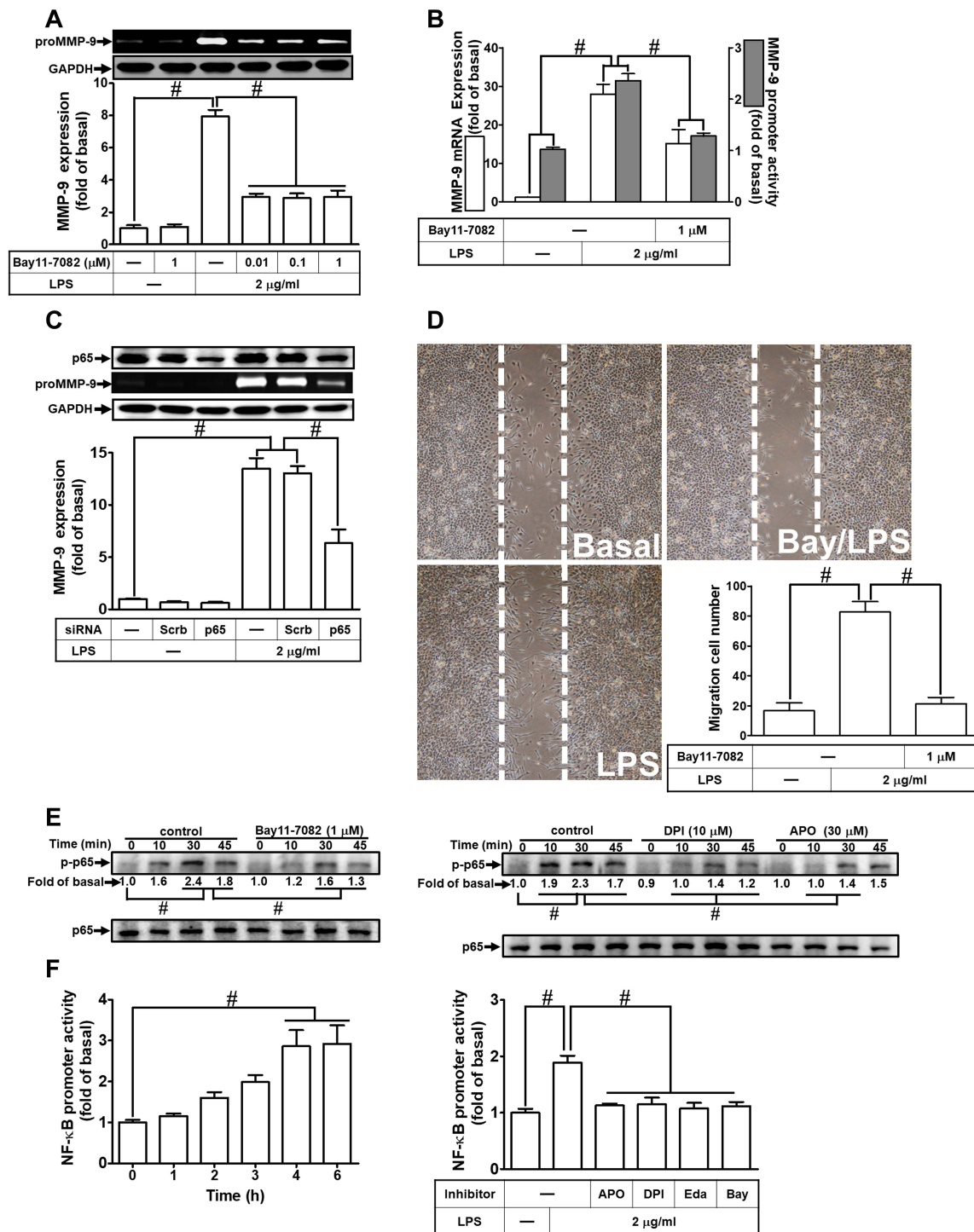


**Figure 4** Nuclear factor-kappa B (NF-κB) is necessary for LPS-induced MMP-9 expression and cell migration in RBA-1 cells. **(A)** Cells were pretreated with Bay11-7082 (0.01, 0.1, and 1 μM) for 1 h and then incubated with LPS (2 μg/mL) for 24 h. The levels of MMP-9 were determined by gelatin zymography. The GAPDH level of cell lysates was assayed by Western blot. **(B)** Cells were pretreated with Bay11-7082 (1 μM) for 1 h and then incubated with LPS (2 μg/mL) of 4 h for mRNA expression or 6 h for promoter activity. The mRNA expression and promoter activity of MMP-9 were determined by real-time PCR and promoter assay, respectively. **(C)** Cells were transfected with Scrb or NF-κB p65 siRNA and then incubated with LPS (2 μg/mL) for 24 h. The medium and cell lysates were collected to determine the levels of MMP-9 by gelatin zymography and the levels of GAPDH and NF-κB p65 by Western blot, respectively. **(D)** Cells were pretreated with Bay11-7082 (1 μM) for 1 h and then incubated with LPS (2 μg/mL) for 48 h. The number of cell migration was determined (magnification = 40×). **(E)** Cells were individually pretreated with or without Bay11-7082 (1 μM), DPI (10 μM), or APO (30 μM) for 1 h and then challenged with LPS (2 μg/mL) for the indicated time intervals (0, 10, 30, and 45 min). The phosphorylation of NF-κB p65 was determined by Western blot. Total NF-κB p65 was analyzed by Western blot used for loading controls. **(F)** Cells were incubated with LPS (2 μg/mL) for indicated time intervals (0, 1, 2, 3, 4, and 6 h) (left panel) or pretreated with or without APO (30 μM), DPI (10 μM), Edaravone (10 μM), or Bay11-7082 (1 μM) for 1 h and then incubated with LPS (2 μg/mL) for 4 h (right panel). NF-κB promoter luciferase activity was detected. Data are expressed as mean ± SEM of three independent experiments. # p < 0.01 as compared with the cells exposed to vehicle or LPS, as indicated.

**Abbreviations:** Eda, edaravone; Bay, Bay11-7082.

NF- $\kappa$ B is involved in the LPS-mediated MMP-9 expression and cell migration in RBA-1 cells.

Next, we explored whether NOS/ROS were upstream signaling molecules of NF- $\kappa$ B p65 in the LPS-mediated signaling pathway. As shown in [Figure 4E](#), we demonstrated that LPS stimulated phosphorylation of NF- $\kappa$ B p65 in a time-dependently manner, which was inhibited by pretreatment with Bay11-7082 (1  $\mu$ M), DPI (10  $\mu$ M), or APO (30  $\mu$ M). Moreover, LPS time-dependently stimulated NF- $\kappa$ B promoter activity ([Figure 4F](#), left panel) which was also attenuated by pretreatment with APO (30  $\mu$ M), DPI (10  $\mu$ M), Edaravone (10  $\mu$ M), or Bay11-7082 (1  $\mu$ M) ([Figure 4F](#), right panel). Finally, we evaluated the binding activity between NF- $\kappa$ B p65 and MMP-9 promoter sequence using a ChIP assay. As shown in [Figure 5A](#), LPS enhanced the binding activity between NF- $\kappa$ B p65 and MMP-9 promoter region in a time-dependent manner (left panel), which was attenuated by pretreatment with Bay11-7082 (1  $\mu$ M), APO (30  $\mu$ M), DPI (10  $\mu$ M), or Edaravone (30  $\mu$ M) (right panel). Upon activation of NF- $\kappa$ B by various stimuli, NF- $\kappa$ B p65 released from I $\kappa$ B complex and translocated into the nucleus, leading to transcription reaction and enhancing the gene expression. As shown in [Figure 5B](#), LPS stimulated NF- $\kappa$ B p65 translocation into the nucleus in a time-dependent manner (left panel), observed by immunofluorescence staining. We further verified whether NOS/ROS regulated the translocation of NF- $\kappa$ B p65 into the nucleus. We observed that the nuclear translocation of NF- $\kappa$ B p65 was blocked by pretreatment with Bay11-7082 (1  $\mu$ M), DPI (10  $\mu$ M), APO (30  $\mu$ M), or edaravone (30  $\mu$ M) (right panel). These results indicated that the NOX/ROS-dependent NF- $\kappa$ B activation mediates LPS-induced MMP-9 expression and cell migration in RBA-1 cells.

## Pristimerin Inhibits LPS-Induced ROS Generation, MMP-9 Expression, and Cell Migration

Pristimerin is one of the triterpenoid compounds. Several lines of literature have reported that pristimerin has anti-inflammation, anti-oxidative stress, and anti-tumorigenesis effects in various types of cells.<sup>16,18</sup> However, whether pristimerin exerted the effects on neuroinflammation is still unknown. First, we checked the cell viability of RBA-1 cells exposed to pristimerin with various concentrations for 24 h. Pristimerin had no significant effect on cell viability except the dose of 1  $\mu$ M ([Figure 6A](#)). Thus, the

concentration of pristimerin used in this study was not higher than 0.5  $\mu$ M. Next, we explored whether pristimerin inhibited the LPS-stimulated ROS generation. The results showed that pretreatment with pristimerin attenuated the LPS-stimulated ROS generation determined by staining with DCFH-DA or DHC in RBA-1 cells ([Figure 6B](#)). Then, we evaluated the effects of pristimerin on the LPS-mediated MMP-9 expression in RBA-1 cells. We found that pretreatment with pristimerin attenuated the LPS-induced MMP-9 expression in a concentration-dependent manner ([Figure 6C](#)). Pristimerin also inhibited MMP-9 mRNA expression ([Figure 6D](#)) and promoter activity ([Figure 6E](#)) induced by LPS in RBA-1 cells. Further, pretreatment with pristimerin also inhibited cell migration of RBA-1 cells challenged with LPS ([Figure 6F](#)). These results indicated that pristimerin could potentially inhibit ROS-dependent MMP-9 expression and cell migration in RBA-1 cells challenged with LPS.

## Pristimerin Attenuates LPS-Mediated NF- $\kappa$ B Activities

According to our present data in RBA-1 cells, we revealed that NF- $\kappa$ B is involved in the LPS-mediated MMP-9 expression. Thus, we evaluated the effects of pristimerin on NF- $\kappa$ B activation in the LPS-challenged RBA-1 cells. First, we found that pretreatment with pristimerin inhibited phosphorylation of NF- $\kappa$ B p65 ([Figure 7A](#)) and promoter activity ([Figure 7B](#)) in RBA-1 cells stimulated by LPS. The nuclear translocation of activated NF- $\kappa$ B p65 was also attenuated by pretreatment with pristimerin, observed by immunofluorescence staining ([Figure 7C](#)). Further, we investigated whether pristimerin attenuated the NF- $\kappa$ B p65 binding with the MMP-9 promoter region. As shown in [Figure 7D](#), pretreatment with pristimerin blocked NF- $\kappa$ B p65 binding to the promoter sequence of MMP-9 in RBA-1 cells stimulated by LPS. These results indicated that pristimerin attenuated LPS-induced MMP-9 expression, at least in part, through decreased NF- $\kappa$ B activity in RBA-1 cells.

## Discussion

In this study, we used pharmacological inhibitors and siRNA transfection to prove that the NADPH oxidase/ROS signaling pathway has a role in LPS-induced MMP-9 expression in RBA-1 cells. Moreover, the signaling conveyed into the nucleus that promoted the activation of transcription factors was defined by immunofluorescent

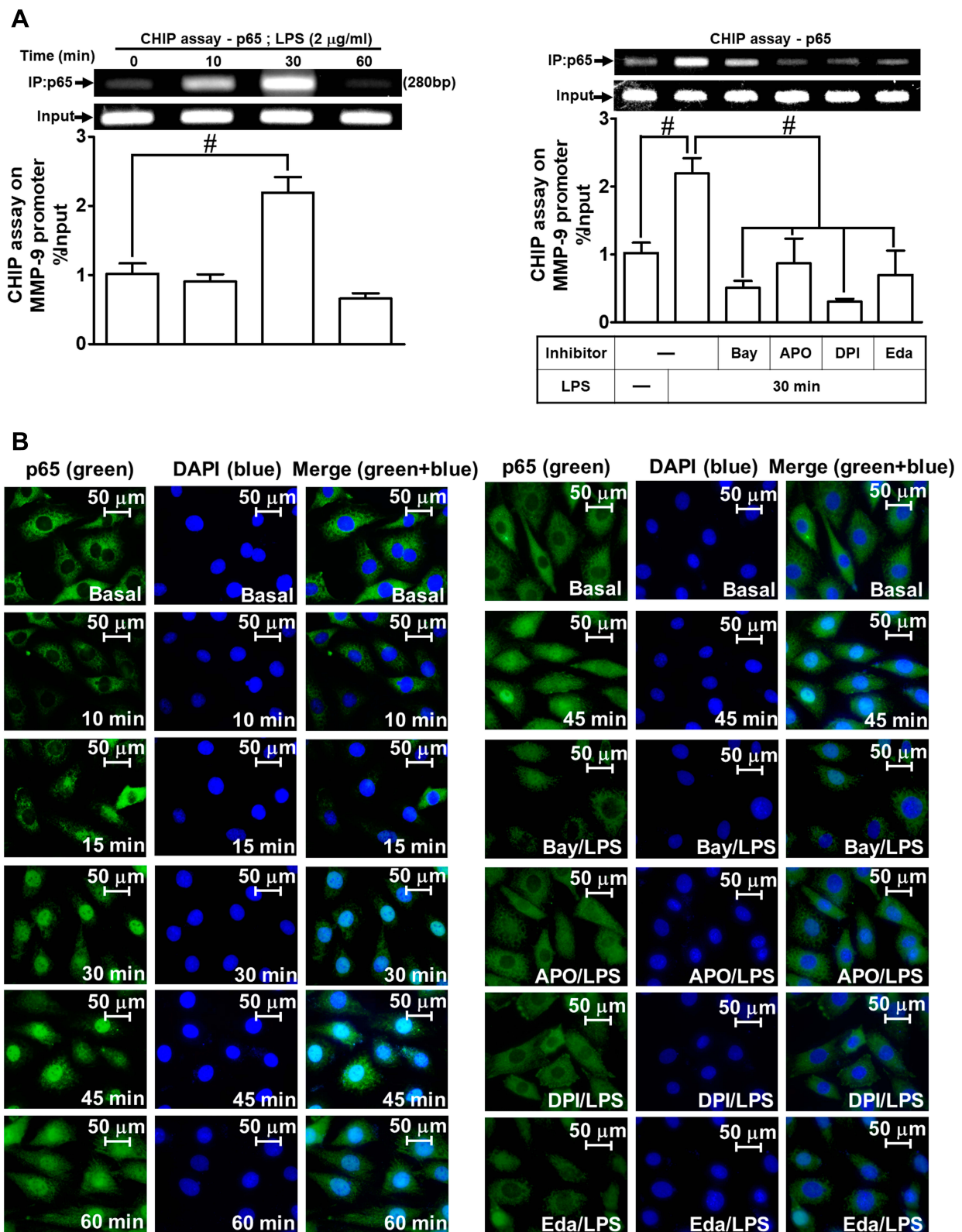


**Figure 5** NF-κB p65 nuclear translocation and binding with MMP-9 promoter element are involved in LPS-induced responses in RBA-1 cells. **(A)** Cells were incubated with LPS (2 µg/mL) for the indicated time intervals (0, 10, 30, and 60 min) (left panel). Cells were pretreated with or without APO (30 µM), DPI (10 µM), Edaravone (30 µM), or Bay11-7082 (1 µM) for 1 h and then incubated with LPS (2 µg/mL) for 30 min (right panel). The levels of NF-κB p65 binding to the MMP-9 promoter element were determined by a chromatin immunoprecipitation (ChIP) assay. **(B)** Cells were incubated with LPS (2 µg/mL) for the indicated time intervals (0, 10, 15, 30, 45, and 60 min). Cells were pretreated with or without APO (30 µM), DPI (10 µM), Edaravone (30 µM), or Bay11-7082 (1 µM) for 1 h and then incubated with LPS (2 µg/mL) for 45 min. The NF-κB p65 nuclear translocation was determined by immunofluorescence staining. The figure represents one of three individual experiments. Scale bar represents 50 µm. Data are expressed as mean ± SEM of three independent experiments. # p < 0.01 as compared with the cells exposed to vehicle or LPS, as indicated.

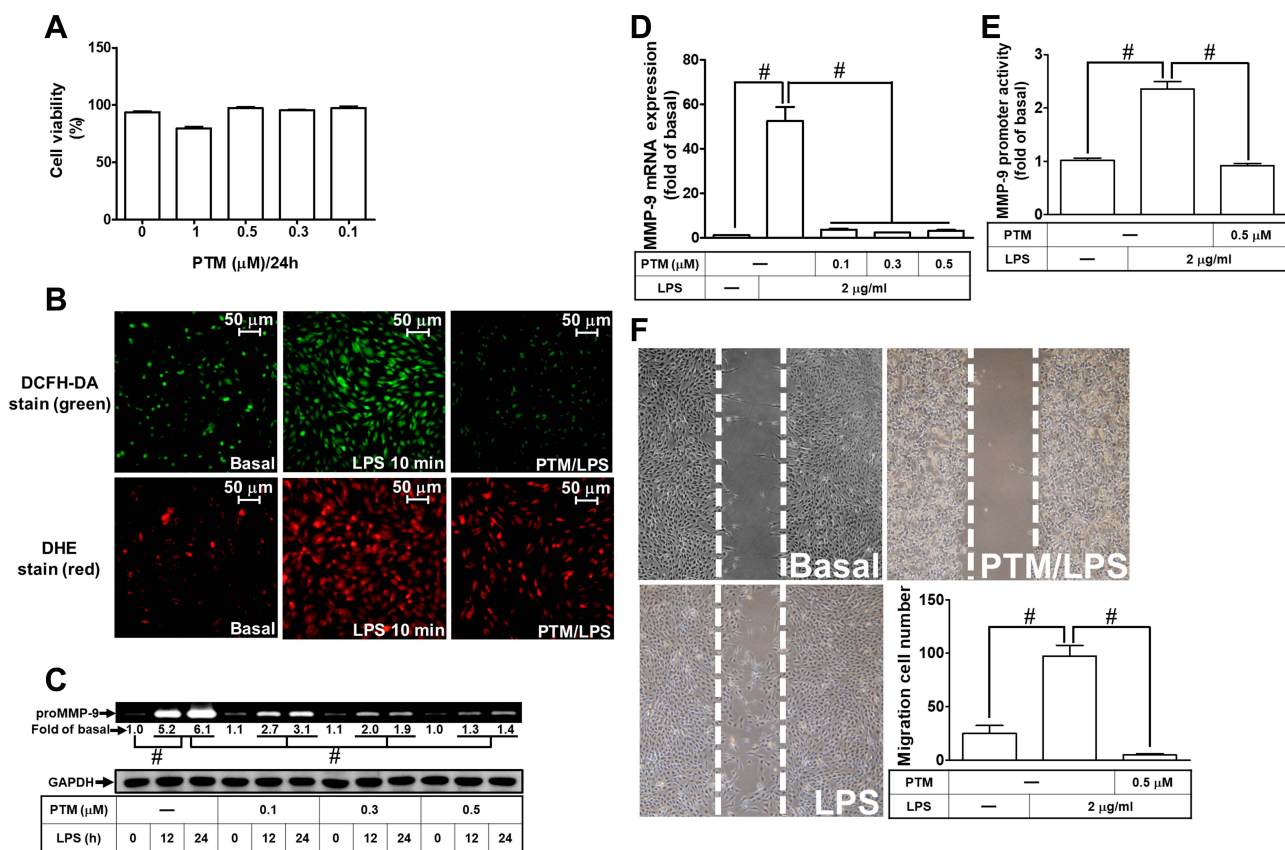


**Figure 6** Pristimerin attenuates ROS generation, proMMP-9 expression, and cell migration induced by LPS in RBA-1 cells. **(A)** The cells were incubated with various concentrations of pristimerin (1, 0.5, 0.3, 0.1  $\mu\text{M}$ ) for 24 h and then cell viability was measured by an XTT assay kit. **(B)** Cells were pretreated with or without pristimerin (0.5  $\mu\text{M}$ ) for 1 h and then incubated with LPS (2  $\mu\text{g}/\text{mL}$ ) for 10 min. The fluorescence intensity of DCFH-DA or DHE staining was detected by a fluorescence microscope. The figure represents one of three individual experiments. Scale bar represents 50  $\mu\text{m}$ . **(C)** Cells were pretreated with or without pristimerin (0.1, 0.3, and 0.5  $\mu\text{M}$ ) for 1 h and then exposed to LPS (2  $\mu\text{g}/\text{mL}$ ) for the indicated time intervals (12 and 24 h). The MMP-9 level was determined by gelatin zymography. The GAPDH level of cell lysates was assayed by Western blot. **(D, E)** Cells were pretreated with or without pristimerin (0.1, 0.3, and 0.5  $\mu\text{M}$  for mRNA expression; 0.5  $\mu\text{M}$  for promoter activity) for 1 h and then incubated with LPS (2  $\mu\text{g}/\text{mL}$ ) of 4 h for mRNA expression or 6 h for promoter activity. The mRNA expression **(D)** and promoter activity **(E)** of MMP-9 were determined by real-time PCR and promoter assay, respectively. **(F)** Cells were pretreated with or without pristimerin (0.5  $\mu\text{M}$ ) for 1 h and then incubated with LPS (2  $\mu\text{g}/\text{mL}$ ) for 48 h. The number of cell migration was determined (magnification = 40 $\times$ ). Data are expressed as mean  $\pm$  SEM of three independent experiments. #  $p < 0.01$  as compared with the cells exposed to vehicle or LPS, as indicated.

**Abbreviations:** XTT, 2,3-bis-(2-methoxy-4-nitro-5-sulphophenyl)-2H-tetrazolium-5-carboxanilide; PTM, pristimerin.

staining and ChIP assay. These results showed that the ROS-dependent pathway contributed to LPS-mediated MMP-9 expression in RBA-1 cells. Furthermore, we also clarified that NOX is a crucial upstream component in regulating the ROS-dependent NF- $\kappa\text{B}$  activity in RBA-1 cells stimulated by LPS. These results suggested that in RBA-1 cells, pristimerin inhibits LPS-induced MMP-9 expression and cell migration via suppressing NOX/ROS-dependent NF- $\kappa\text{B}$  activation.

ROS have been reported to cause neuron damage and enhance inflammatory response in the CNS.<sup>1</sup> Activated glia can produce a large amount of ROS.<sup>31</sup> Several studies have revealed that various neurodegenerative disorders were associated with deleterious effects of ROS production out of control.<sup>1</sup> NOX is a major resource of ROS production. It

has been reported that ROS generated by NOX can lead to MMP-9 expression challenged with various stimuli, including in vivo and ex vivo studies.<sup>32,34</sup> Our results of the present study showed that in RBA-1 cells, NOX-dependent ROS contributes to MMP-9 expression induced by LPS. Moreover, the results were confirmed by ChIP assay, pretreatment of APO, DPI, or edaravone can block the NF- $\kappa\text{B}$  p65 interaction with MMP-9 promoter element. It is consistent with previous reports.<sup>27</sup> Moreover, several reports have shown that scavenging ROS is a candidate for managing neurodegenerative diseases.<sup>34,35</sup> Triterpenoids have been found in a wide range of vegetable kingdom. This kind of compound has many effects on modulating cellular signaling networks including anti-oxidative stress. In this study, we hypothesized that pristimerin, one of the triterpenoids, has

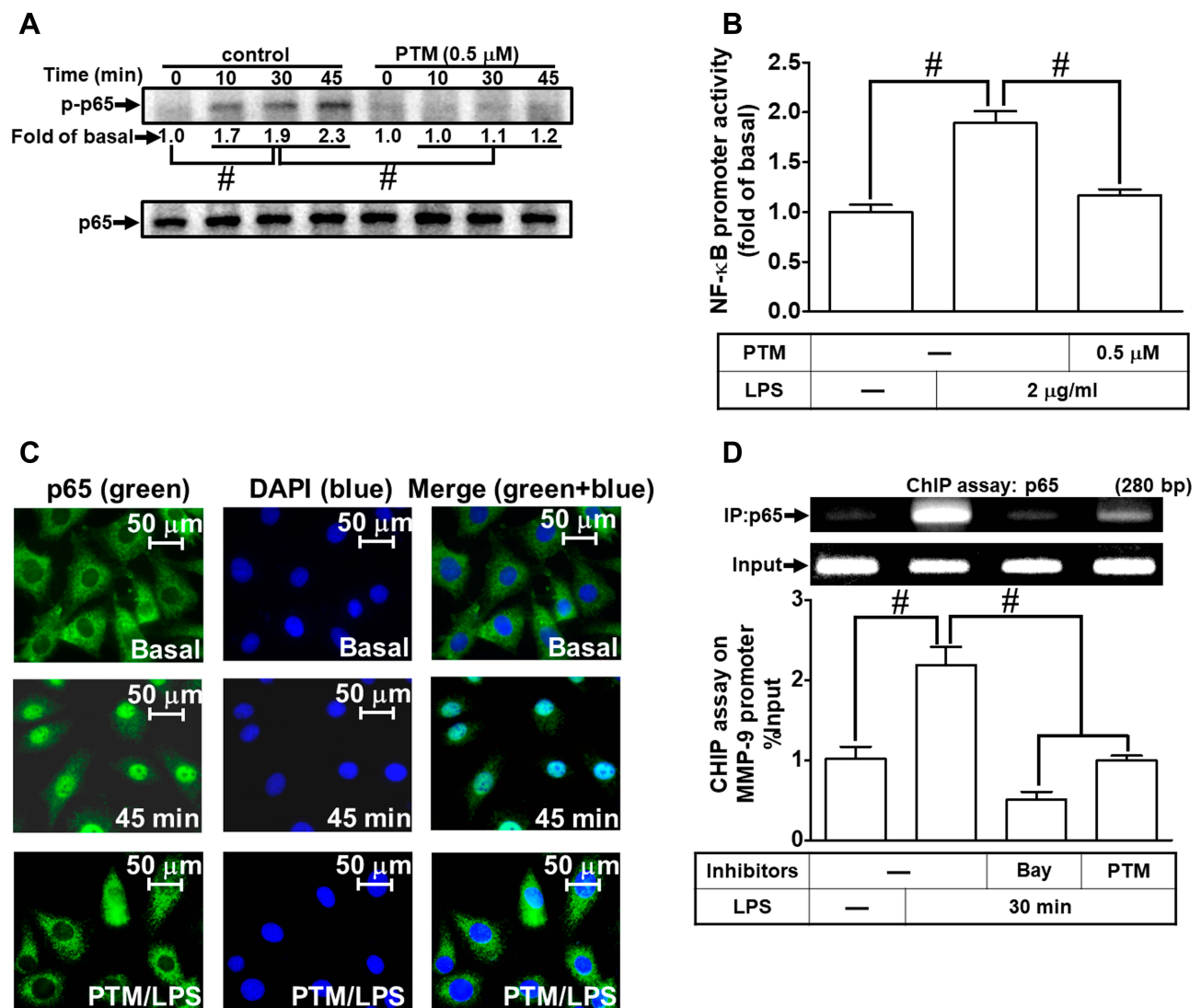


**Figure 7** Pristimerin attenuates LPS-induced NF- $\kappa$ B activity in RBA-1 cells. **(A)** Cells were pretreated with or without pristimerin (0.5  $\mu$ M) for 1 h and then incubated with LPS (2  $\mu$ g/mL) for the indicated time intervals (10, 30, and 45 min). The phosphorylation of NF- $\kappa$ B p65 was detected by Western blot. **(B)** Cells were pretreated with or without pristimerin (0.5  $\mu$ M) and then incubated with LPS (2  $\mu$ g/mL) for 4 h. NF- $\kappa$ B promoter luciferase activity was detected. **(C)** Cells were pretreated with or without pristimerin (0.5  $\mu$ M) for 1 h, and then the LPS-triggered NF- $\kappa$ B p65 nuclear translocation was determined by immunofluorescence staining. The figure represents one of three individual experiments. Scale bar represents 50  $\mu$ m. **(D)** Cells were pretreated with or without pristimerin (0.5  $\mu$ M) or Bay11-7082 (1  $\mu$ M) for 1 h, and then the levels of NF- $\kappa$ B p65 binding with MMP-9 promoter element region triggered by LPS were determined by a ChIP assay. Data are expressed as mean  $\pm$  SEM of three independent experiments. #  $p < 0.01$  as compared with the cells exposed to vehicle or LPS, as indicated.

the effects on scavenging ROS in RBA-1 cells, according to previous literature.<sup>36</sup> Indeed, our results have proved that in RBA-1 cells, pretreatment with pristimerin can scavenge the LPS-mediated ROS generation. Interestingly, some reports showed that pristimerin can induce ROS generation and lead to apoptosis and autophagy on various cancers.<sup>37,39</sup> These opposite phenomena could result from different experimental conditions and cell types.

NF- $\kappa$ B is a transcription factor with a broad range of effects. Many stimuli such as infection, oxidized LDL, ultraviolet irradiation, heavy metals, free radicals, cytokines, and

stress can trigger the activity of NF- $\kappa$ B and contribute to many pathological responses, such as neuroinflammation and neurodegeneration, and physical responses. There have been several reports indicating that NF- $\kappa$ B can modulate MMP-9 expression mediated by various stimuli including LPS.<sup>40,41</sup> In this study, we also hypothesized that in RBA-1 cells, NF- $\kappa$ B was involved in LPS-mediated responses. We found that in RBA-1 cells, LPS can activate NF- $\kappa$ B activity through NOX/ROS signaling pathway to enhance MMP-9 expression. Moreover, our data of NF- $\kappa$ B p65 immunofluorescence staining also revealed that pretreatment of pristimerin can

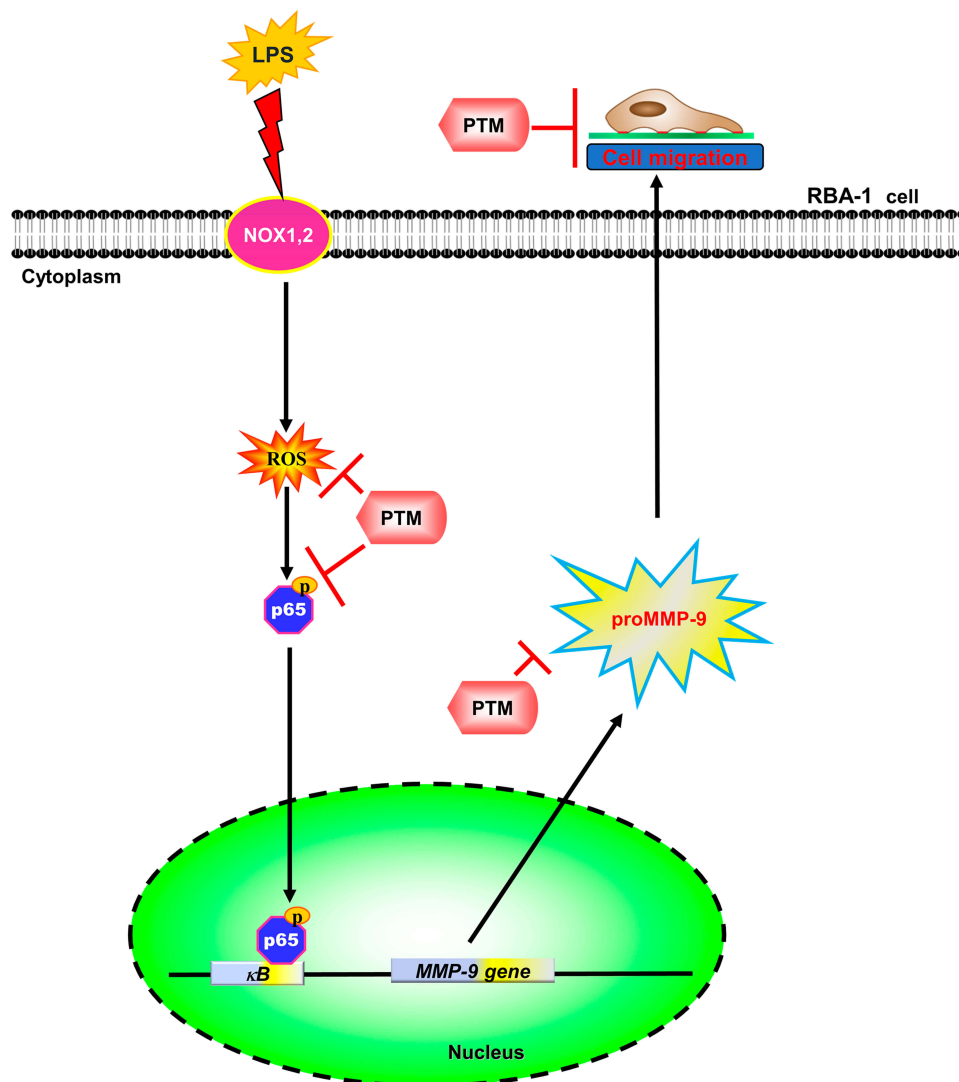


**Figure 8** The schematic signaling pathways are involved in the effects of pristimerin on the LPS-induced MMP-9 expression in RBA-1 cells. Pristimerin blocks NADPH oxidase/ROS generation-dependent p65 nuclear translocation, ultimately leading to attenuating MMP-9 expression and RBA-1 cell migration. “→” means “activated”; “⊥” means “inhibited”.

block NF- $\kappa$ B p65 translocation into the nucleus. The results were confirmed by ChIP assay. Pretreatment with pristimerin can block NF- $\kappa$ B p65 binding with promoter element. This can partially explain the effects of pristimerin on inhibiting LPS-mediated MMP-9 expression.

Hui et al. found that pristimerin inhibited LPS-triggered neurotoxicity through modulating JNK/AP-1 and NF- $\kappa$ B signaling pathways in BV-2 microglia cells.<sup>17</sup> Another study found that pristimerin administration significantly reduced the formation of colonic tumors by decreasing the phosphorylation of AKT and FOXO3a.<sup>18</sup> Deng et al. revealed that pristimerin inhibited VEGF-mediated angiogenesis was via the downregulation of VEGFR2-mediated p-AKT, p-ERK1/2, p-JNK, and

p-p38.<sup>16</sup> It is worth further evaluating the role of receptor tyrosine kinases (RTK), non-RTK, and downstream signaling components on the protective effects of pristimerin in the future. The present study has elucidated, at least partially, the mechanisms by which pristimerin attenuated the expression of inflammatory proteins on RBA-1 cells.

In summary, our results showed that in RBA-1 cells, LPS activated NOX leading to ROS generation, which phosphorylated NF- $\kappa$ B p65, as depicted in Figure 8. Then, p-NF- $\kappa$ B p65 was translocated into the nucleus and was recruited to the promoter region of MMP-9 which increased MMP-9 promoter activity and the expression of MMP-9 mRNA and protein. In turn, the RBA-1 cell migration was enhanced by LPS-mediated MMP-9 expression. Pretreatment with pristimerin

inhibited NOX/ROS-dependent NF- $\kappa$ B activity, which attenuated MMP-9 expression and cell migration in RBA-1 cells challenged with LPS. Therefore, pristimerin can protect LPS-induced neuroinflammatory effects and is a candidate for treating neuroinflammatory and neurodegenerative diseases.

## Conclusions

Here, we verify that in RBA-1 cells, NOX/ROS-dependent NF- $\kappa$ B activity has an important role in LPS-induced MMP-9 expression and cell migration. Further, our results suggest that pristimerin can suppress MMP-9 induction and cell migration induced by LPS in vitro, and its underlying mechanisms are, at least partially, mediated through attenuating the ROS generation and phosphorylation of p65, ultimately lead to blocking p65 translocation, and attenuating NF- $\kappa$ B promoter activity. An advanced understanding of the mechanisms of LPS-mediated inflammatory response and the anti-inflammatory effects of pristimerin may promote the development of potential strategies for neurodegenerative and neuroinflammatory therapeutics.

## Abbreviations

A $\beta$ , amyloid  $\beta$ ; AD, Alzheimer's disease; Ang-1, angiopoietin-1; AP-1, activator protein 1; APO, apocynin; Akt, protein kinase B; BBB, blood-brain barrier; BCA, bichinchonic acid; BK, bradykinin; BSA, bovine serum albumin; CD, cluster of differentiation; ChIP, chromatin immunoprecipitation; CNS, central nervous system; c-Src, proto-oncogene tyrosine-protein kinase; DAPI, 4',6-diamidino-2-phenylindole; DCFH-DA, 2',7'-dichlorodihydrofluorescein diacetate; DHE, dihydroethidium; DMEM, Dulbecco's modified Eagle's medium; DMSO, dimethyl sulfoxide; DPI, diphenyleneiodonium; ECL, enhanced chemiluminescence; EDTA, ethylenediaminetetraacetic acid; ERK1/2, extracellular signal-regulated kinase 1/2; FBS, fetal bovine serum; FOXO, Forkhead box; GAPDH, glyceraldehyde-3-phosphate dehydrogenase; GFAP, glial fibrillary acidic protein; GFP, green fluorescent protein; IKK, I $\kappa$ B-kinase; JNK, c-Jun amino-terminal kinase; LPS, lipopolysaccharide; MAPK, mitogen-activated protein kinase; MMP, matrix metalloproteinase; mTOR, mammalian target of rapamycin; NADPH, nicotinamide adenine dinucleotide phosphate; NF- $\kappa$ B, nuclear factor- $\kappa$ B; NOX, NADPH oxidase; PDGFR, platelet-derived growth factor receptor; PI3K, phosphoinositide 3-kinase; PMSF, phenylmethylsulfonyl fluoride; Pyk2, proline-rich tyrosine kinase; RBA-1, rat brain astrocytes; ROS, reactive oxygen species; SEM, standard error of the mean; SDS, Sodium dodecyl sulfate; TLR, Toll-like receptor; TNF, tumor necrosis factor; VEGF, vascular endothelial

growth factor; XTT, 2,3-bis-(2-methoxy-4-nitro-5-sulfophenyl)-2H-tetrazolium-5-carboxanilide.

## Acknowledgments

We appreciated Chen-yu Wang for his suggestions and construction of plasmids applied in this study and Ya-Fan Shih for her technical assistance.

## Funding

This work was supported by the Ministry of Science and Technology, Taiwan [Grant numbers: MOST107-2320-B-182-020-MY2, MOST108-2320-B-039-061, and MOST108-2320-B-182-014]; China Medical University, Taiwan [Grant numbers: CMU108-MF-08]; and Chang Gung Medical Research Foundation, Taiwan [Grant numbers: CMRPG5F0203 and CMRPG5I0041].

## Disclosure

The authors report no conflicts of interest in this work.

## References

1. Popa-Wagner A, Mitran S, Sivanesan S, Chang E, Buga AM. ROS and brain diseases: the good, the bad, and the ugly. *Oxid Med Cell Longev*. 2013;2013:963520. doi:10.1155/2013/963520
2. Brown GC. The endotoxin hypothesis of neurodegeneration. *J Neuroinflammation*. 2019;16(1):180. doi:10.1186/s12974-019-1564-7
3. Tufekci KU, Genc S, Genc K. The endotoxin-induced neuroinflammation model of Parkinson's disease. *Parkinsons Dis*. 2011;2011:487450. doi:10.4061/2011/153979
4. Zakaria R, Wan Yaacob WM, Othman Z, Long I, Ahmad AH, Al-Rahbi B. Lipopolysaccharide-induced memory impairment in rats: a model of Alzheimer's disease. *Physiol Res*. 2017;66(4):553–565. doi:10.33549/physiolres.933480
5. Zhao J, Bi W, Xiao S, et al. Neuroinflammation induced by lipopolysaccharide causes cognitive impairment in mice. *Sci Rep*. 2019;9(1):5790. doi:10.1038/s41598-019-42286-8
6. Zhan X, Stamova B, Sharp FR. Lipopolysaccharide associates with amyloid plaques, neurons and oligodendrocytes in Alzheimer's disease brain: a review. *Front Aging Neurosci*. 2018;10:42. doi:10.3389/fnagi.2018.00042
7. Zhan X, Stamova B, Jin LW, DeCarli C, Phinney B, Sharp FR. Gram-negative bacterial molecules associate with Alzheimer disease pathology. *Neurology*. 2016;87(22):2324–2332. doi:10.1212/WNL.0000000000003391
8. Asti A, Gioglio L. Can a bacterial endotoxin be a key factor in the kinetics of amyloid fibril formation? *J Alzheimers Dis*. 2014;39(1):169–179. doi:10.3233/JAD-131394
9. Gardner LE, White JD, Eimerbrink MJ, Boehm GW, Chumley MJ. Imatinib methanesulfonate reduces hyperphosphorylation of tau following repeated peripheral exposure to lipopolysaccharide. *Neuroscience*. 2016;331:72–77. doi:10.1016/j.neuroscience.2016.06.007
10. Wang W, Nguyen LT, Burlak C, et al. Caspase-1 causes truncation and aggregation of the Parkinson's disease-associated protein alpha-synuclein. *Proc Natl Acad Sci USA*. 2016;113(34):9587–9592. doi:10.1073/pnas.1610099113

11. Yang CC, Lin CC, Hsiao LD, Kuo JM, Tseng HC, Yang CM. Lipopolysaccharide-induced matrix metalloproteinase-9 expression associated with cell migration in rat brain astrocytes. *Int J Mol Sci*. 2019;21(1):259. doi:10.3390/ijms21010259
12. Lee EJ, Ko HM, Jeong YH, Park EM, Kim HS. Beta-lapachone suppresses neuroinflammation by modulating the expression of cytokines and matrix metalloproteinases in activated microglia. *J Neuroinflammation*. 2015;12(1):133. doi:10.1186/s12974-015-0355-z
13. Rosenberg GA. Matrix metalloproteinases in neuroinflammation. *Glia*. 2002;39(3):279–291. doi:10.1002/glia.10108
14. Park SK, Hwang YS, Park KK, Park HJ, Seo JY, Chung WY. Kalopanaxaponin A inhibits PMA-induced invasion by reducing matrix metalloproteinase-9 via PI3K/Akt- and PKCdelta-mediated signaling in MCF-7 human breast cancer cells. *Carcinogenesis*. 2009;30(7):1225–1233. doi:10.1093/carcin/bgp111
15. Weiss N, Miller F, Cazaubon S, Couraud PO. The blood-brain barrier in brain homeostasis and neurological diseases. *Biochim Biophys Acta*. 2009;1788(4):842–857. doi:10.1016/j.bbamem.2008.10.022
16. Deng Q, Bai S, Gao W, Tong L. Pristimerin inhibits angiogenesis in adjuvant-induced arthritic rats by suppressing VEGFR2 signaling pathways. *Int Immunopharmacol*. 2015;29(2):302–313. doi:10.1016/j.intimp.2015.11.001
17. Hui B, Zhang L, Zhou Q, Hui L. Pristimerin inhibits LPS-triggered neurotoxicity in BV-2 microglia cells through modulating IRAK1/ TRAF6/TAK1-mediated NF-kappaB and AP-1 signaling pathways in vitro. *Neurotox Res*. 2018;33(2):268–283. doi:10.1007/s12640-017-9837-3
18. Park JH, Kim JK. Pristimerin, a naturally occurring triterpenoid, attenuates tumorigenesis in experimental colitis-associated colon cancer. *Phytomedicine*. 2018;42:164–171. doi:10.1016/j.phymed.2018.03.033
19. El-Agamy DS, El-Harbi KM, Khoshhal S, et al. Pristimerin protects against doxorubicin-induced cardiotoxicity and fibrosis through modulation of Nrf2 and MAPK/NF-kB signaling pathways. *Cancer Manag Res*. 2019;11:47–61. doi:10.2147/CMAR.S186696
20. Jou TC, Jou MJ, Chen JY, Lee SY. Properties of rat brain astrocytes in long-term culture. *Taiwan Yi Xue Hui Za Zhi*. 1985;84(8):865–881.
21. Wu CY, Hsieh HL, Jou MJ, Yang CM. Involvement of p42/p44 MAPK, p38 MAPK, JNK and nuclear factor-kappa B in interleukin-1beta-induced matrix metalloproteinase-9 expression in rat brain astrocytes. *J Neurochem*. 2004;90(6):1477–1488. doi:10.1111/j.1471-4159.2004.02682.x
22. Eberhardt W, Schulze M, Engels C, Klasmeier E, Pfeilschifter J. Glucocorticoid-mediated suppression of cytokine-induced matrix metalloproteinase-9 expression in rat mesangial cells: involvement of nuclear factor-kappaB and Ets transcription factors. *Mol Endocrinol*. 2002;16(8):1752–1766. doi:10.1210/me.2001-0278
23. Wu CY, Hsieh HL, Sun CC, Tseng CP, Yang CM. IL-1 beta induces proMMP-9 expression via c-Src-dependent PDGFR/PI3K/Akt/p300 cascade in rat brain astrocytes. *J Neurochem*. 2008;105(4):1499–1512. doi:10.1111/j.1471-4159.2008.05318.x
24. Hsu HY, Wen MH. Lipopolysaccharide-mediated reactive oxygen species and signal transduction in the regulation of interleukin-1 gene expression. *J Biol Chem*. 2002;277(25):22131–22139. doi:10.1074/jbc.M111883200
25. Wei P, Yang F, Zheng Q, Tang W, Li J. The potential role of the NLRP3 inflammasome activation as a link between mitochondria ROS generation and neuroinflammation in postoperative cognitive dysfunction. *Front Cell Neurosci*. 2019;13:73. doi:10.3389/fncel.2019.00073
26. Dias V, Junn E, Mouradian MM. The role of oxidative stress in Parkinson's disease. *J Parkinsons Dis*. 2013;3(4):461–491. doi:10.3233/JPD-130230
27. Kim SY, Lee JG, Cho WS, et al. Role of NADPH oxidase-2 in lipopolysaccharide-induced matrix metalloproteinase expression and cell migration. *Immunol Cell Biol*. 2010;88(2):197–204. doi:10.1038/icb.2009.87
28. Liu J, Iwata K, Zhu K, et al. NOX1/NADPH oxidase in bone marrow-derived cells modulates intestinal barrier function. *Free Radic Biol Med*. 2019;147:90–101. doi:10.1016/j.freeradbiomed.2019.12.009
29. Lin CC, Hsieh HL, Shih RH, et al. NADPH oxidase 2-derived reactive oxygen species signal contributes to bradykinin-induced matrix metalloproteinase-9 expression and cell migration in brain astrocytes. *Cell Commun Signal*. 2012;10(1):35. doi:10.1186/1478-811X-10-35
30. Rosenberg GA. Matrix metalloproteinases and their multiple roles in neurodegenerative diseases. *Lancet Neurol*. 2009;8(2):205–216. doi:10.1016/S1474-4422(09)70016-X
31. Akinrinade ID, Memudu AE, Ogundele OM, Ajetonmobi OI. Interplay of glia activation and oxidative stress formation in fluoride and aluminium exposure. *Pathophysiology*. 2015;22(1):39–48. doi:10.1016/j.pathophys.2014.12.001
32. Yang CM, Hsieh HL, Yu PH, Lin CC, Liu SW. IL-1beta Induces MMP-9-dependent brain astrocytic migration via transactivation of PDGF receptor/NADPH oxidase 2-derived reactive oxygen species signals. *Mol Neurobiol*. 2015;52(1):303–317. doi:10.1007/s12035-014-8838-y
33. Yang CM, Lee IT, Hsu RC, Chi PL, Hsiao LD. NADPH oxidase/ROS-dependent PYK2 activation is involved in TNF-alpha-induced matrix metalloproteinase-9 expression in rat heart-derived H9c2 cells. *Toxicol Appl Pharmacol*. 2013;272(2):431–442. doi:10.1016/j.taap.2013.05.036
34. Velimirovic M, Jevtic Dozudic G, Selakovic V, et al. Effects of vitamin D3 on the NADPH oxidase and matrix metalloproteinase 9 in an animal model of global cerebral ischemia. *Oxid Med Cell Longev*. 2018;2018:3273654. doi:10.1155/2018/3273654
35. Yang CC, Lin CC, Jou MJ, Hsiao LD, Yang CM. RTA 408 inhibits interleukin-1beta-induced MMP-9 expression via suppressing protein kinase-dependent NF-kappaB and AP-1 activation in rat brain astrocytes. *Int J Mol Sci*. 2019;20(11):2826. doi:10.3390/ijms20112826
36. Hui B, Yao X, Zhou Q, Wu Z, Sheng P, Zhang L. Pristimerin, a natural anti-tumor triterpenoid, inhibits LPS-induced TNF-alpha and IL-8 production through down-regulation of ROS-related classical NF-kappaB pathway in THP-1 cells. *Int Immunopharmacol*. 2014;21(2):501–508. doi:10.1016/j.intimp.2014.06.010
37. Zhao Q, Liu Y, Zhong J, et al. Pristimerin induces apoptosis and autophagy via activation of ROS/ASK1/JNK pathway in human breast cancer in vitro and in vivo. *Cell Death Discov*. 2019;5(1):125. doi:10.1038/s41420-019-0208-0
38. Liu Y, Ren Z, Li X, et al. Pristimerin induces autophagy-mediated cell death in K562 cells through the ROS/JNK signaling pathway. *Chem Biodivers*. 2019;16(8):e1900325. doi:10.1002/cbdv.201900325
39. Liu YB, Gao X, Deeb D, Arbab AS, Gautam SC. Pristimerin induces apoptosis in prostate cancer cells by down-regulating Bcl-2 through ROS-dependent ubiquitin-proteasomal degradation pathway. *J Carcinog Mutagen*. 2013;(Suppl 6):005.
40. Yang CC, Lin CC, Chien PT, Hsiao LD, Yang CM. Thrombin/matrix metalloproteinase-9-dependent SK-N-SH cell migration is mediated through a PLC/PKC/MAPKs/NF-kappaB cascade. *Mol Neurobiol*. 2016;53(9):5833–5846. doi:10.1007/s12035-015-9485-7
41. Yang CC, Lin CC, Hsiao LD, Yang CM. Galangin inhibits thrombin-induced MMP-9 expression in SK-N-SH cells via protein kinase-dependent NF-kappaB phosphorylation. *Int J Mol Sci*. 2018;19(12):4084. doi:10.3390/ijms19124084



## Journal of Inflammation Research

Dovepress

### Publish your work in this journal

The Journal of Inflammation Research is an international, peer-reviewed open-access journal that welcomes laboratory and clinical findings on the molecular basis, cell biology and pharmacology of inflammation including original research, reviews, symposium reports, hypothesis formation and commentaries on: acute/chronic inflammation; mediators of inflammation; cellular processes; molecular

mechanisms; pharmacology and novel anti-inflammatory drugs; clinical conditions involving inflammation. The manuscript management system is completely online and includes a very quick and fair peer-review system. Visit <http://www.dovepress.com/testimonials.php> to read real quotes from published authors.

Submit your manuscript here: <https://www.dovepress.com/journal-of-inflammation-research-journal>